

Development of Sintering Materials by Sea Sediments and TiO₂ for the Cleaning Technology

Mohammad Arifur Rahman,^{1*} Satoshi Kaneco,² Tohru Suzuki,³ Hideyuki Katsumata,² Kiyohisa Ohta² and A. M. Shafiqul Alam¹

¹Department of Chemistry, University of Dhaka, Dhaka-1000, Bangladesh

²Department of Chemistry for Materials, Faculty of Engineering, Mie University, Tsu, Mie 514-8507, Japan

³Environmental Preservation Center, Mie University, Tsu, Mie 514-8507, Japan

Abstract

A solar decontamination process for water was developed using photocatalysts supported on sea bottom sediments with sodium silicate. The supported catalysts were systematically optimized with respect to TiO₂ dosages, calcinations temperature and binder dosages. The Young's Modulus value (compressed strength) was found 12.5 kN/mm² of optimized supported catalyst which would not mixed with the water of real samples during the photocatalysis. The composition of the optimized catalyst was selected as sediments 82%, TiO₂ 15% and Na₂SiO₃ 3%, where the sintering temperature was 750°C. Humic acid as a model compound was used to evaluate the degradation efficiency of the developed sintering material. The complete mineralization of humic acid was achieved by 40 h sunlight irradiation. About 100 ml of (15 mg/L) of humic acid was successfully degraded with 15 g sintering materials under sunlight irradiation. The solar photocatalytic degradation treatment is simple, easy handling and cheap. Therefore, since the artificial lamp devices, for example Hg-Xe lamp, are particularly expensive in the local and nonexclusive areas, the optimized developed sintering material appears to be very suitable treatment method for humic acid in those area.

Introduction

In recent years, the use of wide band-gap semiconductors, such as TiO₂, as photocatalyst has aroused great interest in particular as a promising technique for remediation of environmental pollution in both liquid and gas phase reaction [1]. Ultraviolet (UV) illumination of a semiconductor photocatalyst in an aqueous solution establishes a redox environment capable of degrading organic chemicals. As in other AOPs, hydroxyl radicals (OH) are thought to be the primary oxidants responsible for the degradation of organic contaminants in photocatalysis [2].

The well-known principle of photooxidation is that UV illumination onto a photocatalyst excites to produce electron and hole pair (e⁻/h⁺) with high energy state, which migrate the particle surface and initiate a wide range of chemical reactions [3]. The valence band potential is positive enough to generate hydroxyl radicals at the surface and the conduction band potential

is negative to reduce molecular oxygen. The hydroxyl radical is used as a powerful oxidizing agent to convert organic pollutants into CO₂, H₂O, and less toxic byproducts of a low molecular weight.

Ultra fine TiO₂ powders have large specific surface areas, and good catalytic activities since reactions take place on the TiO₂ surface. However, powders easily agglomerate into larger particles, resulting in an adverse effect on catalyst performance [4]. It is also very hard to recover pure TiO₂ powders from water when they are used in aqueous systems [5]. Alternatively, the catalyst may be immobilized onto a suitable solid support matrix which would eliminate the need for post-treatment removal.

Several different methods for the immobilization of TiO₂ on solid support substrate have been investigated by other researchers. TiO₂ powder was immobilized on solid support substrates (stainless steel, titanium alloy, titanium metal, and tin oxide

*Corresponding Author E-mail: marahman76@yahoo.com

coated glass) using electrophoretic coating and spray coating [6] J. -C. Lee et al., 2000 used three kinds of TiO₂ immobilization on the glass tube of the UV lamps by a sol-gel method and a hydrothermal method [7]. A. Danion et al., 2004 built a TiO₂-coated optical fibre photoreactor by sol-gel method. M [8]. Bideau et al., 1995 used glass beads [9], R. W. Matthews & H. Al-Ekabi et al., 1988 investigated glass tubing substrates [9-11]. Y. Zhang et al., 1994 used sand, silica gel, glass beads, glass fiber mesh, glass wool fiber to prepare immobilized TiO₂ by dip coating from suspension [12]. A. Fernandez et al., 1995 used quartz and H. Tada et al., 1995 used optical fibers by sol gel related methods [13, 14].

To the best of our knowledge, there has been no work about the development of sintering materials by sea sediments and anatase TiO₂ with different sintering temperatures (400-800°C). H. Wang et al., 2005 [15] synthesized anatase TiO₂ by drying in supercritical ethanol (7.0 MPa, 270°C) and calcinations at high temperature and found with increasing of the calcinations temperature up to 800°C, the photocatalytic activities were increased gradually. Anatase TiO₂ is the thermodynamically metastable and can be easily transformed into the stable rutile phase when it is heated to 500-600°C. Moreover, anatase TiO₂ with higher crystalliteslinity is preferred for photocatalysis, since the higher crystalliteslinity would mean fewer defects for the recombination of photogenerated electrons and holes. Extensive studies of the effect of Al₂O₃, SiO₂, ZrO₂ and Al₂O₃-SiO₂ additives on the phase transformation of TiO₂ by J. Yang et al., 1997 & 1998 and J. Kim et al., 2001 showed that the additives functioned to retard the anatase-to-rutile phase transformation [16,17]. Since the sea bottom sediments of Ago Bay, Japan contain 51.09(Wt.%) SiO₂ and 16.54(Wt.%) Al₂O₃ etc. [18], the sea bottom sediments with TiO₂ would not change the anatase-to-rutile phase transformation during sintering temperatures.

The objective of the present research was to develop the sintering materials by sea bottom sediments and TiO₂ with different temperatures and compositions for the degradation of organic pollutant such as humic acid [19-22].

Experimental

The sea bottom sediments were dredged and collected in July, 2004 where SiO₂ 51.09%, Al₂O₃ 16.54%, CaO 13.41%, Fe₂O₃ 5.63%, K₂O 3.52%, SO₄ 3.32%, MgO 2.35%, Na₂O 1.58% and TiO₂ 0.57% were the main chemical components [18], and it also contained 40% H₂O. An electric oven (Koyo Box Furnace, KBF828N, Nara, Japan) was used for the

sintering in the range of 500 to 800°C under air atmosphere. Firstly, sodium silicate (in technical grade) and TiO₂ powder (anatase, purity 99.9%, diameter 230 nm, surface area 8.7 m²/g, Wako Pure Chemical Industries, Ltd., Osaka) were added to the sea bottom sediments. The photocatalytic activity, intrinsic photocatalytic activity and specific photocatalytic activity of TiO₂ is 0.135 m⁻¹ min⁻¹, 0.196 (m⁻¹ min⁻¹ m⁻²) and 10.8 m⁻¹min⁻¹ g⁻¹ respectively [23]. Sodium silicate was added as a binder material. Ultra pure water 20 mL, which was purified by an ultra pure water system (Advantec MFS Inc., Tokyo, Japan, resulting in a resistivity > 18 MΩ cm) was added and mixed together to get a uniform mixture. Then it was air-dried for 15 minutes in room temperature. After 15 minutes, small balls (about 0.5 cm diameter) were prepared by hand with the sediments mixture. Again, the balls were air-dried for 24 hours for initial setting. A variety of mixture ratios of the sea bottom sediments, TiO₂ and sodium silicate were used to prepare the sintered products represented in the Table 1.

Table 1. Composition of the sintering materials

Material Code	Composition % (Wt)	Sintering temperature/°C
m ₁	Sediments 95 / TiO ₂ 5	500,550,600,650,700,750 & 800
m ₂	Sediment 90 / TiO ₂ 10	500,550,600,650,700,750 & 800
m ₃	Sediment 85 / TiO ₂ 15	500,550,600,650,700,750 & 800
m _{1a}	Sediments 90 / TiO ₂ 5 / Na ₂ SiO ₃ 5	500,550,600,650,700,750 & 800
m _{1b}	Sediments 85 / TiO ₂ 5 / Na ₂ SiO ₃ 10	500,550,600,650,700,750 & 800
m _{1c}	Sediments 80 / TiO ₂ 5 / Na ₂ SiO ₃ 15	500,550,600,650,700,750 & 800
m _{1d}	Sediments 92 / TiO ₂ 5 / Na ₂ SiO ₃ 3	700,750 & 800
m _{2a}	Sediments 85 / TiO ₂ 10 / Na ₂ SiO ₃ 5	500,550,600,650,700,750 & 800
m _{2b}	Sediments 80 / TiO ₂ 10 / Na ₂ SiO ₃ 10	500,550,600,650,700,750 & 800
m _{2c}	Sediments 75 / TiO ₂ 10 / Na ₂ SiO ₃ 15	500,550,600,650,700,750 & 800
m _{2d}	Sediments 87 / TiO ₂ 10 / Na ₂ SiO ₃ 3	700,750 & 800
m _{3a}	Sediments 80 / TiO ₂ 15 / Na ₂ SiO ₃ 5	500,550,600,650,700,750 & 800
m _{3b}	Sediments 75 / TiO ₂ 15 / Na ₂ SiO ₃ 10	500,550,600,650,700,750 & 800
m _{3c}	Sediments 70 / TiO ₂ 15 / Na ₂ SiO ₃ 15	500,550,600,650,700,750 & 800
m _{3d}	Sediments 82 / TiO ₂ 15 / Na ₂ SiO ₃ 3	700,750 & 800

The air dried products were then sintered by electric oven with temperatures. The sintering temperature increased from ordinary temperature to the final one at 20°C/min, and then the temperature was kept constant for 4h. The special cylindrical shaped sintering products were prepared which were 10 mm in length and 5 mm in diameter for strength (stability) measurements of the materials with variation of composition and temperature. The specimens were made in the metal moulds with open tops. The moulds were made in such a way that the side walls and the base of the form work were detachable so that the mould could be easily separated from the specimens after its initial setting. The requisite amount of sediments, TiO₂ and Na₂SiO₃ were mixed dry in a pan, and then the requisite quantity of water was added gradually while the mixture was continuously stirred. Then, the moulds were air-dried for 48 hours for initial setting. After that the air dried products were then sintered by electric oven. In order to measure the strength (stability) of the sintering products, universal testing machine (Capacity 50 ton, Marui and Co. Ltd. Osaka, Japan) and set up was followed according to the reference [24].

In order to evaluate the degradation capacity, the sintered products were applied to the humic acid solution (prepared by Wako Pure Chemical Industries, Ltd. Osaka). Photochemical experiments were performed in a 50 mL cylindrical Pyrex reaction vessel with a diameter of 3.2 cm and a height of 8.0 cm. The degradation experiments were performed using usual batch system. A solution of (30 mL) of humic acid was mixed with 15 g (8 pieces) of sintered materials. The sintering materials with humic acid were irradiated under sunlight illumination. In this case, the short ultraviolet radiation ($\lambda < 300$ nm) was filtered out by the vessel wall. The intensity of light was measured by a UV radio meter with a sensor of 320 to 410 nm wave lengths (UVR-400, Iuchi Co., Osaka, Japan). The light intensity of most of the sunny days was 1.5-1.9 mW/cm². The variations of sunlight intensity for 60 min were less than 10%.

After illumination, sintering materials were separated through the 110 mm Advantec filter. The clear solution was measured using a UVIDE 610/650 double-beam spectrometer (JASCO Co., Japan) with a resonance of 254 and 436 nm. Humic acid concentration at 436 nm was measured to check the colour forming moieties that are the chromophoric groups containing conjugated double bond systems (delocalized electrons).

Results and discussion

According to Ollis et al. and Link [25, 26],

the major obstacle to the implementation of photocatalysis is the engineering of cost-effective reactors. Reactors that employ a catalyst suspended in slurry and catalyst fixed on support are two major reactor options. As far as continuous flow operation is concerned, a number of investigators have reported the degradation of various organic compounds with fixed bed reactors [27-30]. Despite the previous successful use of supported catalysts, it is thought that mass transfer limitation might outweigh the advantages of a fixed catalyst [24]. Matthews used coiled tube reactors coated with and without TiO₂ to compare performances of slurry and supported catalysts [26]. For most of solutes tested, the degradation rates of slurries were found higher than those of supported catalysts. In our research, sun light irradiated photocatalysis by developed sintering materials also showed the lower degradation rate compare to slurry.

Because photocatalysis is an extremely complicated process, systematic investigations, such as sintering temperature, dosages of TiO₂ and binder materials, and strength (stability) of the materials are required to develop a convenient, cheap and widely applicable photocatalyst for the degradation of organic pollutants in water.

Development and optimization of Supported photocatalysts

Control and Dark Experiments

The adsorption of molecules onto a surface is a necessary prerequisite to any surface mediated chemical process. Therefore, the binding of humic acid to the sintering materials has to be addressed in order to improve the understanding of photocatalytic degradation. It is known that the initial adsorption kinetics of humic acids on solid surfaces is rather a complex process that depends on nature of the surface and the solution conditions [27]. In the first experiment, the reactors were packed with the variety of sintering materials (m_1 , m_2 & m_3) with the humic acid solution (15 mg/L, 30 mL, pH 7.0) and these were kept in the dark room for 8h. After an establishment of the equilibrium between humic acid and sintering materials, its (HA) concentrations were measured at 254 nm and 436 nm wavelength by UV-Visible spectrophotometer. It was observed that 50-60% and 40-50% humic acid was remained in the equilibrium solution at 254 and 436 nm resonances respectively. It means that 40-50% humic acid was adsorbed by the surface of the sintering materials after 8 h. The pH of the equilibrium solution was varied from 7.0~7.2 for 700, 750 and 800°C of sintered materials (m_1 , m_2 & m_3) but the pH 7.5~8.0 was also observed for 500 to 650°C of sintered materials.

This might be due to the leaching of some alkali metals from those sintered materials.

Sunlight irradiated experiment

The degradation of HA was monitored under sunlight irradiation with various sintering materials. **Figure 1**, showed that lower the percentage of sodium silicate, appreciable degradation (C/C_0 at 254 nm) was obtained with the materials of higher sintering temperature (m_{1a}), however material (m_1) showed higher efficiency of HA degradation. **Figure 2**, showed the results at 436 nm wavelength where m_{1a} and m_1 proved almost similar degradation (C/C_0) efficiency. From the **Figure 1** and **Figure 2**, it was concluded that the lower percentage of sodium silicate higher percentage of degradation capacity by the sintering materials.

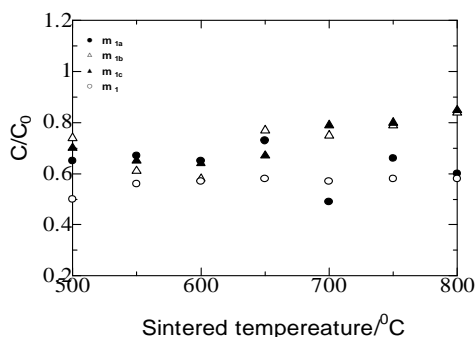


Figure 1. Photocatalytic degradation of HA (254 nm) by sintering materials.

HA concentration: 15 mg/L
 TiO₂ in sintering material: 5 (wt %)
 Sintering temperature: 500~800°C
 Na₂SiO₃ in sintering material: 5~15 (Wt %)
 Amount of sintered material: 15.0 g
 Irradiation time: 8 h, No. of experiments: n = 3

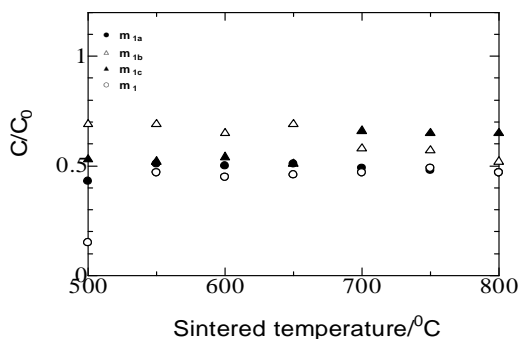


Figure 2. Photocatalytic degradation of HA (436 nm) by sintering materials.

HA concentration: 15 mg/L
 TiO₂ in sintering material: 5 (wt %)
 Sintering temperature: 500~800°C
 Na₂SiO₃ in sintering material: 5~15 (Wt %)
 Amount of sintered material: 15.0 g
 Irradiation time: 8 h, No. of experiments: n = 3

Here, the percentage of TiO₂ was constant in every composition of the materials but temperature, binder and sediments percentages were varied. From this experiment, it was clear that not only TiO₂ percentage but other compositional changes also responsible for the degradation of HA in water.

Since the lower percentage of binder into the sintering materials favored the degradation of HA acid, another new composition (sediments 87% + TiO₂ 10% + Na₂SiO₂ 3%) was included in the degradation experiments. Sintering material m_{2d} and m_2 at 254 nm wave length have higher degradation efficiency at higher sintering temperature than other sintering materials. Moreover, the degradation capacities were not dependent with the titanium percentages as shown in **Figure 3**. At sintering temperature of 700, 750 and 800°C shown lower values of C/C_0 than other sintered materials, presented in **Figure 4**. However, in the **Figure 3** and **Figure 4**, only the degradations of HA with m_{2d} checked at 700, 750 and 800°C temperature. Because the materials with lower sintering temperature (500 to 650°C) were partially broken during the degradation experiments and deposited onto the bottom of the experimental flasks. This was not desirable for the ideal photocatalytic degradation experiments.

In order to optimize the TiO₂ in the sintering materials, higher percentages of photocatalysts were added. At higher sintering temperature, higher degradation rate was found by m_{3d} and m_3 shown in the **Figure 5** and **Figure 6** at 254 and 436 nm resonances respectively. At 750°C sintering temperature, most of the sintering materials showed a high degree of degradation at 254 nm. Moreover, at 800°C and 750°C of sintering temperature, the materials (m_{3d} , m_{3c} and m_3) have the maximum degradation efficiency at 436 nm, where colour forming moieties degraded by sintered materials with sunlight irradiation. This result indicating that lower the percentages of binder or without the binder has proven to be its great degradation efficiency. Since we need a harder sintering material, lower percentages of sodium silicate containing sintering materials would enhance its durability and longest life time.

From the above mentioned Figures, it is clear that higher amount of photo-catalyst, higher degree of degradation efficiency. Since, TiO₂ is very lighter than the sediments; addition of titanium oxide (more than 15% wt) with the sediments was not possible, which agglomerate onto the surface of sintering products. As a results, the sintering products were become very soft than our desired materials due to the lacking of uniformity. Sintering materials which were sintered at a temperature of 400, 450°C also checked for the

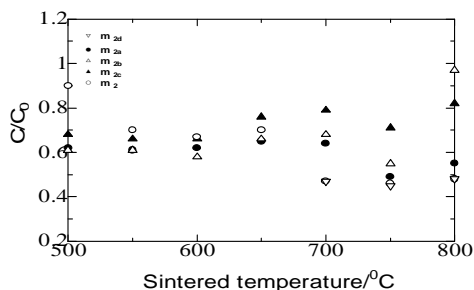


Figure 3. Photocatalytic degradation of HA (254 nm) by sintering materials.

HA concentration: 15 mg/L
 TiO₂ in sintering product: 10 (wt %)
 Sintering temperature: 500~800°C
 Na₂SiO₃ in sintering material: 3~15 (Wt %)
 Amount of sintered material: 15.0 g
 Irradiation time: 8 h, No. of experiments: n = 3

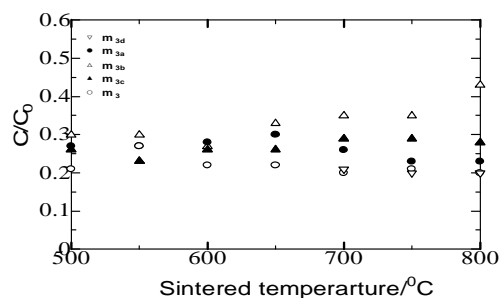


Figure 6. Photocatalytic degradation of HA (436 nm) by sintering materials.

HA concentration: 15 mg/L
 TiO₂ in sintering material: 15 (Wt %)
 Sintering temperature: 500~800°C
 Na₂SiO₃ in sintering material: 3~15 (Wt %)
 Amount of sintered material: 15.0 g
 Irradiation time: 8 h, No. of experiments: n = 3

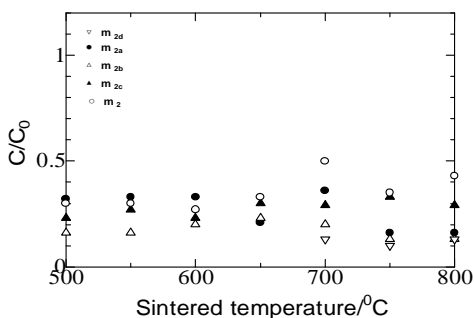


Figure 4. Photocatalytic degradation of HA (436 nm) by sintering materials.

HA concentration: 15 mg/L
 TiO₂ in sintering material: 10
 Sintering temperature: 500~800°C
 Na₂SiO₃ in sintering material: 3~15 (Wt %)
 Amount of sintered material: 15.0 g
 Irradiation time: 8 h, No. of experiments: n = 3

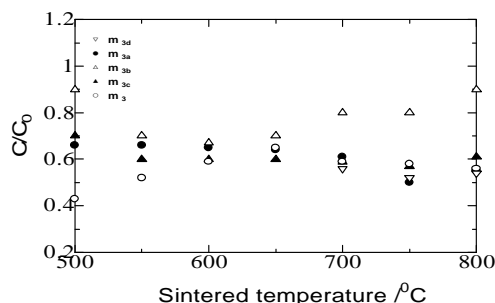


Figure 5. Photocatalytic degradation of HA (254 nm) by sintering materials.

HA concentration: 15 mg/L
 TiO₂ in sintering material: 15 (Wt %)
 Sintering temperature: 500~800°C
 Na₂SiO₃ in sintering material: 3~15 (Wt %)
 Amount of sintered material: 15.0 g
 Irradiation time: 8 h, No. of experiments: n = 3

degradation of HA. After addition of sintering materials into the humic acid solution, the pH of degraded solution increased. This was because of the sintering materials which was broken partially and deposited on the bottom of the experimental flask.

The Photocatalytic activity of TiO₂ of the prepared materials depended strongly on the temperature used to anneal the photocatalyst. Annealing of TiO₂ above 600°C caused considerable sintering of the particles, and thus decreases in surface area [28]. The degradation of HA by sintering materials at lower sintering temperature (500, 550, 600°C) showed also better degradation efficiencies compared to other sintering temperature. This is because of the anatase form of TiO₂ crystals in the sintering products. Generally, above 600°C temperature, the photodegradation decreases due to the rutile formation of TiO₂ crystals. In this experiment, above 600°C of sintering temperature proved higher degree of degradation, which might be due to the larger amount of SiO₂ and Al₂O₃ in the sediments retarded the anatase-to-rutile phase transformation. Kim et al. and Yang et al. studied extensively the effects of Al₂O₃, SiO₂, ZrO₂ and Al₂O₃-SiO₂ additives on the phase transformation of TiO₂ and showed that the additives functioned to retard anatase-to-rutile phase formation [17, 15, 16].

pH of the degraded solution

After 8h sunlight irradiation, the pH of the degraded solution was measured. **Figure 7**, showed that increasing of sodium silicate percentages in the sintering materials also increased the pH value of the degraded solution. At higher sintering temperature (700, 750 and 800°C), the pH of the degraded solutions were

lower in most of the sintering materials. Presumably, it may be due to the strongly attachment of the Na_2SiO_3 with the sediments at higher temperature. After Photocatalytic degradation by m_1 , the pH values of the degraded solution were nearly 7.0 at higher sintering temperature. But at the same temperature, the pH values increased with the Na_2SiO_3 percentages. These results indicated that Na_2SiO_3 produced sodium hydroxide into the humic acid solution that increased the pH of the solution. On the other hand, almost the same types of pH observed in **Figure 8** and **Figure 9**. Since lower sintering temperature materials produced high pH into the degraded solution, only sintering materials of 700, 750 and 800°C sintering temperature were checked for 3% Na_2SiO_3 with variation of TiO_2 .

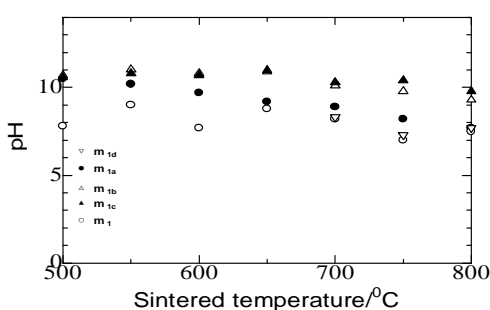


Figure 7. Change of pH after sunlight irradiation.

HA concentration: 15 mg/L
 TiO_2 in sintering material: 5 (Wt %)
 Sintering temperature: 500~800°C
 Na_2SiO_3 in sintering material: 3~15 (Wt %)
 Amount of sintered material: 15.0 g
 Irradiation time: 8 h, No. of experiments: n = 3

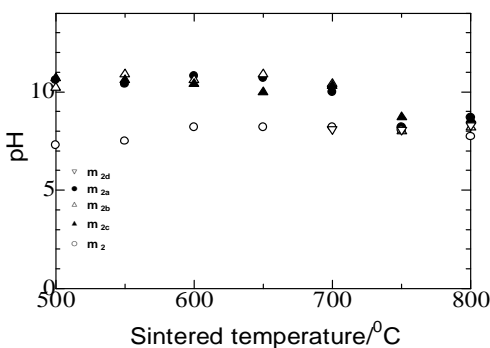


Figure 8. Change of pH after sunlight irradiation.

HA concentration: 15 mg/L
 TiO_2 in sintering material: 10 (Wt %)
 Sintering temperature: 500~800°C
 Na_2SiO_3 in sintering material: 3~15 (Wt %)
 Amount of sintered material: 15.0 g
 Irradiation time: 8 h, No. of experiments: n = 3

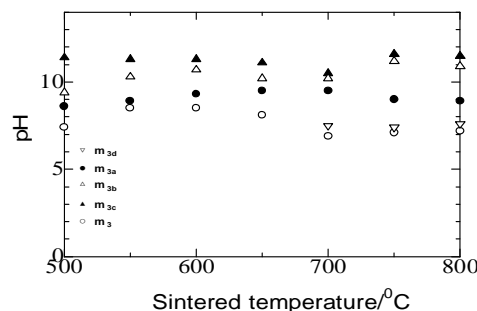


Figure 9. Change of pH after sunlight irradiation.

HA concentration: 15 mg/L
 TiO_2 in sintering material: 15 (Wt %)
 Sintering temperature: 500~800°C
 Na_2SiO_3 in sintering material: 3~15 (Wt %)
 Amount of sintered material: 15.0 g
 Irradiation time: 8 h, No. of experiments: n = 3

Considering the pH_{zpc} of anatase TiO_2 as pH 6.3-6.6 and the pH of the reaction medium (7.0), the role of electrostatic attractions should be considered as significant during the course of adsorption process. In the dark experiments, most of the sintering materials adsorbed about 50% humic acid after 8h. The experiment was carried out at neutral pH. This might be the physical adsorption of the rough surfaces of sintering materials along with chemical adsorption of TiO_2 . The degradation of HA also checked under sunlight irradiation as shown in Figure 1 to Figure 6, where the initial pH of HA solution was almost neutral. At $\text{pH} < 6.3$, the positively charge $\text{TiO}_2\text{-H}^+$ offer suitable surface for negatively charged HA molecular adsorption, but at $\text{pH} > 6.3$, the surface of TiO_2 become negatively charged $\text{TiO}_2(\text{OH})^-$ which provide an unfavorable condition for the HA molecule to approach. Under neutral pH conditions, humic acid should be considered an anion that is partially charged due to the deprotonation of the carboxylic groups present at the periphery of the molecules. Then, the surface $-\text{OH}_2^+$ and $-\text{OH}$ groups might exchange with the anionic groups of humic acid through ligand exchange mechanism [31-33].

Adsorption spectrum of the humic acid

After 8h sunlight irradiation of humic acid with sintering materials, the degradation spectrum was checked as shown in **Figure 10**. Three types of sintering materials were applied for the degradation of HA under sunlight irradiation. From the **Figure 10**, it is clearly proved that the developed sintering materials have the efficiencies to degrade the humic acid under sunlight irradiation. It suggested that least amount (5~3%) of sodium silicate would not be involved for the degradation mechanism. At 436 nm, HA absorption was

lower than 254 nm region in the **Figure 10**. The reason may be attributed to the higher removal rate of color forming moieties with higher percentages of TiO₂ present in the sintering materials. But in the UV region around 200 nm, the absorption peak was higher than the peak of standard humic acid solution after sunlight irradiation.

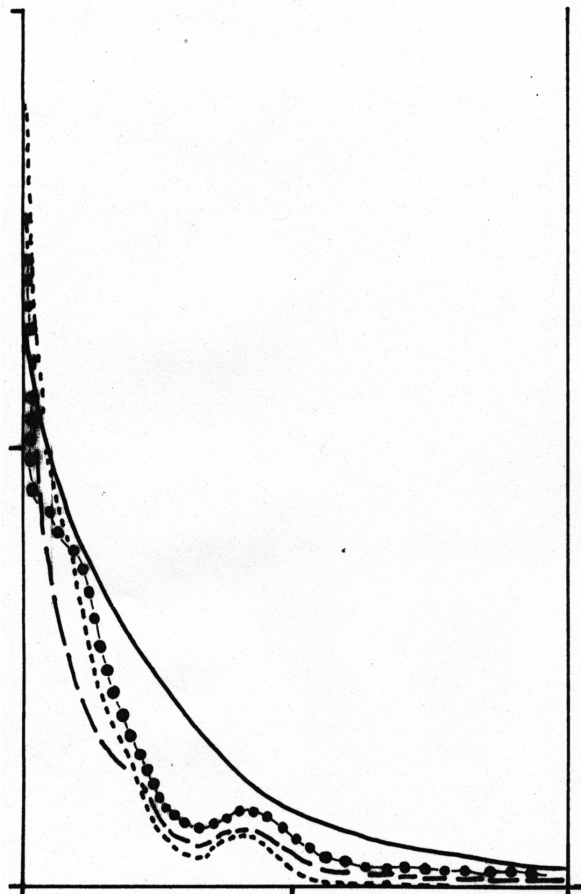


Figure 10. Change of HA spectrum after sunlight irradiation.

HA concentration: 15 mg/L
 TiO₂ in sintering product: 5~15 (Wt %)
 Sintering temperature: 750°C
 Na₂SiO₃ in sintering material: 5 (Wt %)
 Amount of sintered material: 15.0 g
 Irradiation time: 8 h, No. of experiments: n = 3

This indicates the degradation of high molecular size of humic acid to lower molecular weight compounds which increased the percentages of aromaticity in the solution showed higher absorption peak than the original one. After 8 h sunlight irradiation, there were unusual peaks found in the visible wavelength region (about 350 nm wave length). It might be due to the complicated adsorptive process of humic acid onto the sintering materials surfaces. Since TiO₂

surface was hydrophilic and should be considered as not favorable for the adsorption of hydrophobic organic compounds, the aromatic moieties of humic acid extended to the bulk of the solution. Therefore, the aromatic moieties and with the other leached metals in the solution formed another complexes.

The Photocatalytic activity of sintering materials for the degradation of humic acid was very slow since the mineralization was not completed within 8 h sunlight irradiation. This decrease in photoactivity by sintering materials correlated mostly with the decrease of surface area of the TiO₂ particles and not with the anatase to rutile transformation which occurred only above 700°C. Moreover, under neutral pH conditions, HA likely to be assumed more extended (linear) conformations because of the hydrophilicity of the polar functional groups and the mutual repulsion of the ionized groups. Due to the huge molecular size of humic acids, rearrangements in the adsorbed humic acid molecule with the newly arriving ones of larger mass, and the desorption of the former photoreacted fractions lead to extreme surface heterogeneity forming microinterfaces within the adsorbed layer. This case lowers the probability of the reactivity of the photogenerated holes through direct charge transfer thereby resulting in oxidation rates [33].

Photodegradation efficiency with volume of humic acid

Sintering material (m_{3d}) showed higher efficiency than any other sintering products. In order to apply this developed material to the rivers, lakes and sea, m_{3d} was selected as an ideal sintering material for the degradation of humic acid. Photodegradation efficiency of sintering materials with different volume of same concentration of humic acid was checked. With increasing of volume of humic acid degradation efficiency was decreased. Moreover, the degradation efficiency pattern was not changed with time. It might be due the lower contacts rate between the TiO₂ surfaces and the molecule of HA with higher volume of same concentration (15 mg/L). Additionally, it was a batch process which was performed without stirring/shaking of the solution. From this finding, it was clear that higher volume of same concentration of HA could degrade but took longer time than expected. From this experiment, it was observed that 30-100 mL HA was degraded with 15g of sintering materials. Alternatively, 45g, 75g of sintering materials would be required in order to get better degradation efficiency of 300 mL and 500 mL of HA of the same concentration respectively. It suggests that according to the volume and concentration of HA in ponds, lakes, rivers and seas, the amounts of sintering materials will be selected.

Mineralization of humic acid

From the previous efficiency experiment, 100 mL (15 mg/L) of humic acid was selected for the mineralization with m_{3d} sintering material. In the **Figure 12**, the degradation rate was high within 8h sunlight irradiation, after that it became slow. About 60% of the humic acid was degraded by 8h and it was continued slowly to degrade completely by 40h. It is known that the initial adsorption kinetics of humic acids on solid surfaces is rather complex process. Moreover, with time, the accessibility of active sites on the surface could be limited as a result of steric blockage by humic macromolecules. As a result, the degradation rates became slowed down. This experiment was carried out five times ($n=5$) where the deviation of the results was found 7~10%.



Figure 12. Mineralization with the developed & optimized sintering materials

HA concentration: 15 mg/L (100 mL)
 TiO₂ in sintering material: 15 (Wt %)
 Sintering temperature: 750°C
 Na₂SiO₃ in sintering material: 3 (Wt %)
 Amount of sintered material: 15.0 g, No. of experiments: $n=5$

Strength of the sintering products

The strength will play a vital role in the selection of composition and sintering temperature for construction of sintering materials for the degradation of HA in the water. In view of taking account this important factor, few sintering materials were selected and compressed strengths (stability) were measured which was given in **Table 2**. The results showed that lower the sintering temperatures and the percentage of sodium silicate, lower the Young's Modulus, kN/mm² values (lower the stability of the sintering materials). According to our previous degradation experiments and also considering these strength values, m_{3d} (prepared with 750°C sintering temperature) was selected for the

degradation of HA in the water which Young's Modulus value (strength) was 12.5 kN/mm² as presented in **Table 2**. The compressed strengths of different sintering materials were quite reasonable since sodium silicate is a binder material and high sintering temperature would also increased more bonding characteristics between the sediments, TiO₂ and Na₂SiO₃.

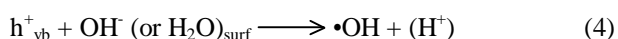
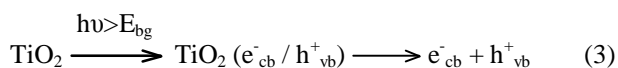
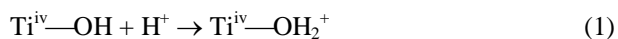
Table 2. Compressive Strength of the different sintering materials (kN/mm²).

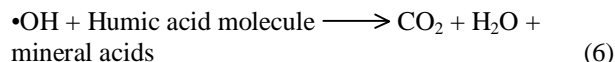
Material Code	Sintering temperature/°C	Average Young's Modulus, kN/mm ²
m_{3d}	500	6.5
m_{3d}	600	7.2
m_{3d}	700	10.5
m_{3d}	750	12.5
m_{3d}	800	13.2
m_{3a}	750	13.5
m_{3b}	750	14.0
m_{3c}	750	14.7
m_3	750	7.3

No. of measurements $n=2$

Degradation mechanism and kinetics

At neutral pH, the surface of the TiO₂ is equally positively and negatively charged according to the reaction (1) and (2). Then humic acid adsorbed through ion exchange mechanism by the surface of TiO₂ since humic acid was considered as anion due to the deprotonation from its carboxylic groups. After that the photoreactions proceed by the UV absorption from the sunlight. It is known that upon UV irradiation, TiO₂ particles generate electron-hole pairs (e^-_{CB}/h^+_{VB}) in the bulk semiconductor which can migrate to the surface to form oxidizing species (HOO^\bullet , $O_2^{\bullet-}$ and then $^\bullet OH$ radicals) via reacting with preadsorbed O₂. These radical species possess a potential to oxidize humic acid molecules at the TiO₂ surface presented in the sintering materials and produce 4-hydroxybenzoic acid, oxalic acid, succinic acid and malonic acid [33]. Although the main pathway of photo mineralization may easily be summarized by the reaction below (3-6), the detailed mechanisms of the photocatalytic oxidation process at the TiO₂ surface keep being elusive, about the initial steps involve in the reactions of HOO^\bullet , $O_2^{\bullet-}$ and $^\bullet OH$ radicals with the humic acid:





It has been documented that an increase the crystallization degree of anatase TiO₂ can usually lead to an enhancement in its catalytic activity for the Photocatalytic degradation of organic pollutants in air and wastewater [34-37]. The enhancement of Photocatalytic activity is often ascribed to that highly crystallized anatase TiO₂ would have less defects acting as the recombination centers for photogenerated electrons and holes. But in this experiment, the photodegradation by the developed sintering materials was slower than photodegradation of humic acid by TiO₂ powder [33, 37, 38]. Since sediments in sintering products contained SiO₂ 51.09% and Al₂O₃ 16.54% which helped to retard anatase-to-rutile phase formation [15-17]. It might be due to the decreased of surface area of TiO₂ particles by high sintering temperature and not with the anatase to rutile formation. Annealing of TiO₂ above 600°C caused considerable sintering of the particles and thus decreased the surface area [26]. As a consequence, the adsorption of humic acid on the catalyst surface was less which would help to concentrate the reactant molecules for the photoreactions and the photos might be scattered in between the TiO₂ particles, causing the photoreactions more easy to happen.

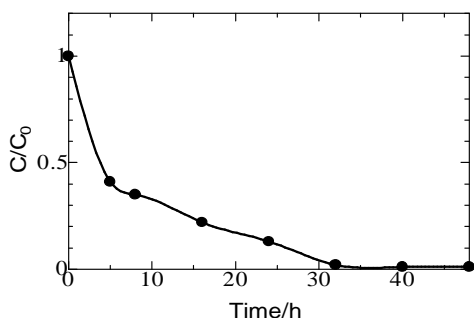


Figure 11. Degradation efficiency of sintering materials with change of HA volume.

Irradiation time: ● (8 h); □ (16 h); ▲ (24 h); ○ (32 h); ◻ (40 h); ▼ (48 h)

HA concentration: 15 mg/L

TiO₂ in sintering material: 15 (Wt %)

Sintering temperature: 750°C

Na₂SiO₃ in sintering material: 3 (Wt %)

Amount of sintered material: 15.0 g, No. of experiments: n = 3

The rate of photocatalytic degradation of HA over illuminated TiO₂ could be explained with the Langmuir-Hinshelwood (L-H) kinetic expression [32]. Moreover, the degradation of HA over illuminated TiO₂

followed first order kinetics and the activation energy was 17 KJ mol⁻¹ [33]. However, the usual activation energies for organic photocatalysis are 5 -16 KJ mol⁻¹. The observed activation energy indicates a lower effect of the temperature on the photocatalytic degradation of HA. The effect of temperature on the rate of oxidation may be dominated by the rate of interfacial electron transfer to oxygen [32].

Conclusion

A simple, cheap and convenient supported photocatalyst was developed as presented in the Figure 13 and promising options were identified. All the optimization experiments were carried out three times (n=3) and the deviation of the results was found 8~12%. Greater degradation efficiency was observed with m_{3d} than the other sintering materials. The rate of degradation of HA was slower compared to TiO₂ slurry. But this sintering material would be applied in the pond, lakes, rivers and seas where sunlight could reach and the degradation time would not be a vital factor. Generally, TiO₂ powders easily agglomerate into larger particles, resulting in an adverse effect on catalyst performance; however, there is no possibility to be agglomerate of the catalyst powders in the developed sintering material. Moreover, the catalyst would not mix with the water which is the most advances of this developed sintering material and would be very easy to recover as a pure TiO₂. Since the artificial lamp device for photocatalytic degradation is particularly expensive in the nonexclusive areas, and the dredged sea bottom sediments are available everywhere in the world, therefore, this sintering material would be able to have an application potential for the degradation of organic pollutants in water under sunlight irradiation to protect the water environment.

References

1. D. M. Blake, RREL/TP-430-22197, National Renewable Energy Laboratory, Golden Co., (1997/1999).
2. Y. Zhang, J. C. Crittenden, D. W. Hand and D. L. Perram, *Environ. Sci. Technol.* 28, (1994) 435.
3. H. R. Hoffmann, S. T. Martin, W. Choi and D. W. Bahnemann, *Chem. Rev.* 95 (1995) 69.
4. H. Y. Zhu, J. -Y. Li, J. -C. Zhao and G. J. Churchman, *Appl. Clay Sci.* 28 (2005) 79.
5. D. Beydoun, R. Amal, G. K. -C. Low and S. McEvoy, *J. Phys. Chem. B* 104 (2000) 4387.
6. J. A. Byrne, B. R. Eggins, N. M. D. Brown, B. Mckinney and M. Rose, *Appl. Catal. B. Environ.* 17 (1998) 25.
7. J, -C. Lee, M. -S. Kim and B. -W. Kim, *Water Res.* 36 (2002) 1776.

8. A. Danion, J. Disdier, C. Guillard, F. Abdelmalek and N. J.-Renault, *Appl. Catal. B.* 52 (2004) 213.
9. M. Bideau, B. Claudel, C. Dubin and L. Faure, Kazouan, *J. Photochem. Photobiol. A. Chem.* 91 (1995) 137.
10. R. W. Matthews, *Catal.* 111 (1988) 264.
11. H. Al-Ekabi and N. Serpone, *J. Phys. Chem.* (1988) 5726.
12. Y. Zhang, J. C. Crittenden and D. W. Hand, *Chem. Ind.* 18 (1994) 714.
13. G. Fernandez, G. Lassaletta, V. M. Jimenez, A. Justo, A. R. Gonzalez-Eliphe, Herrmann, H. Tahiri and Y. Ait-Ichcou, *Appl. Catal. B.* 7 (1995) 49.
14. H. Tada and H. Honda, *J. Electrochem. Soc.* 25 (1995) 1169.
15. J. Yang, Y. X. Huang and F. M. F. Ferreira, *J. Mater. Sci. Lett.* 16 (1997) 1933.
16. [J. Yang and F. M. F. Ferreira, *J. Mater. Lett.* 36 (1998) 320.
17. J. Kim, K. C. Song, S. Foncillas and S. E. Pratsinis, *J. Eur. Ceram. Soc.* 21 (2001) 2863.
18. S. Kaneco, T. Harada, A. H. A. Dabwan, T. Suzuki, H. Katsumata and K. Ohta, *ITE Lett. Batt. New Technol. Med.* 5 (2004) 33.
19. I. Christl and R. Kretzschmar, *Environ. Sci. Technol.*, 41 (2007) 1915.
20. J. Buschmann, A. Kappeler, U. Lindauer, D. Kistler, M. Berg and L. Sigg, *Environ. Sci. Technol.* 40 (2006) 6015.
21. C. Lamelas and V. I. Slaveykova, *Environ. Sci. Technol.*, 41 (2007) 4172.
22. S. Kaneco, R. Furuo, M. A. Rahman, T. Suzuki, H. Katsumata and K. Ohta., *Photo/Electrochem & Photobiol. Environ. Energy Fuel*, (2005) 399.
23. M. Bekbolet, A. S. Suphandag and C. S. Uyguner, *J. Photochem. Photobiol. A. Chem.*, 148 (2002) 121.
24. M. Z. Hossain and S. Inoue, *J. Sci. Israel-Technol. Advan.*, 6 (2004) 81.
25. D. F. Ollis, E. Pelizzetti and N. Serpone, *Environ. Sci. Technol.* 25 (1991) 1522.
26. H. Link, Solar Energy Research Institute (SERI): Golden, Co, (1990).
27. N. Serpone, E. Borgarello, R. Harris, P. Cahill and M. Borgarello, *Sol. Energy Mater.* 14 (1986) 121.
28. R. W. Matthews, *Sol. Energy*, 38 (1987) 405.
29. W. R. Matthews, *Water Res.* 25 (1991) 1169.
30. R. W. Matthews, *Water Res.* 24 (1990) 653.
31. M. J. Avena and L. K. Koopal, *Environ. Sci. Technol.* 33 (1999) 2739.
32. A. Mills and S. Morris, *J. Photochem. Photobiol. A. Chem.*, 71 (1993) 285.
33. R. Al-Rasheed and D. J. Cardin, *Chemosphere.* 51 (2003) 925.
34. B. Ohtani and S. Nishimoto, *J. Phys. Chem.* 97 (1993) 920.
35. J. Ovenstone, *J. Mater. Sci.* 36 (2001) 1325.
36. H. Kominami, J. Kato, S. Y. Murakami, Y. Ishii, M. Kohno, K. Yabutani, T. Yamamoto, Y. Kera, M. Inoue, T. Inui and B. Ohtani, *Catal. Today.* 84 (2003) 181.
37. J. G. Yu, H. G. Yu, B. Cheng,; X. J. Zhao, J. C. Yu and W. K. Ho, *J. Phys. Chem. B.* 107 (2003) 13871.
38. J. Wiszniowski, D. Robert, J. Surmacz-Gorska, K. Mirneliusz and J. -V. Weber, *J. Photochem. Photobiol. A. Chem.*, 152 (2002) 267.